Molecular Docking and ADME Profiling of N-(Substituted-1,3-benzothiazol-2-yl)benzamide Derivatives as Potential Anticonvulsant Agents

Ahmed Rufa'i[1*], Abdullahi Y. Idris[2], Aliyu M. Musa[2], Halimatu S. Hassan[2], Asma'u H. Nasiru[2], Mohammed G. Magaji[3], Rabiu Bako[4], Muhammad Sa'idu[5], Isah J. Muhammad[6]

[1]Department of Pharmaceutical and Medicinal Chemistry, Faculty of Pharmaceutical Sciences, Gombe State University, Gombe, Nigeria.

[2]Department of Pharmaceutical and Medicinal Chemistry, Faculty of Pharmaceutical Sciences, Ahmadu Bello University, Zaria, Nigeria.

[3]Department of Pharmacology and Therapeutics, Faculty of Pharmaceutical Sciences, Ahmadu Bello University, Zaria, Nigeria.

[4]Department of Pharmaceutical and Medicinal Chemistry, Faculty of Pharmaceutical Sciences, Kaduna State University, Kaduna, Nigeria.

[5]Department of Pure and Applied Chemistry, Faculty of Physical Sciences, Kaduna State University, Kaduna, Nigeria.

[6]Department of Pharmaceutical and Medicinal Chemistry, Faculty of Pharmaceutical Sciences, Ibrahim Badamasi Babangida University, Lapai, Niger, Nigeria.

[*]**Corresponding author name**: Ahmed Rufa'i

[*]**Corresponding author. E-mail**: roofmoon4cool@gmail.com, Tel: +2347068296718

Affiliation and Address: Department of Pharmaceutical and Medicinal Chemistry, Faculty of Pharmaceutical Sciences, Gombe State University, Gombe, Nigeria.

Abstract

Amides represent a class of organic compounds with a variety of biological potential and anticonvulsant properties.This study aimed to evaluate the pharmacokinetic properties and molecular interactions of 15 N-(substituted-1,3-benzothiazol-2-yl)benzamide derivatives with

two key epilepsy-related targets, γ-aminobutyric acid aminotransferase (GABA-AT) and activated open sodium ion channel proteins, in order to assess their potential anticonvulsant activity. Crystal structures of GABA-AT (PDB ID: 1OHW) and the sodium ion channel (PDB ID: 5HVX) were obtained from the RCSB Protein Data Bank. Molecular docking was performed using AutoDock Vina following protein preparation in Chimera v1.11.2. Post-docking analysis was conducted using Chimera and Discovery Studio Visualizer. ADME properties were also predicted. ADME analysis showed high gastrointestinal absorption for all compounds except compound 5. Docking results revealed that seven compounds (Cp1, Cp3, Cp7, Cp10, Cp12, Cp13, and Cp14) exhibited interaction profiles similar to vigabatrin, while three (Cp10, Cp13, and Cp14) aligned with lamotrigine. These compounds demonstrated favorable binding interactions with both targets. The docking analysis suggest that selected N-(substituted-1,3-benzothiazol-2-yl)benzamide derivatives, particularly Cp1, Cp3, Cp7, Cp10, Cp12, Cp13, and Cp14 were identified as the most promising lead candidates, with significant potential for anticonvulsant activity.

Keywords: Activated open sodium ion channel; amides; ADME; epilepsy; GABA-AT; *in-silico* studies.

Graphical Abstract

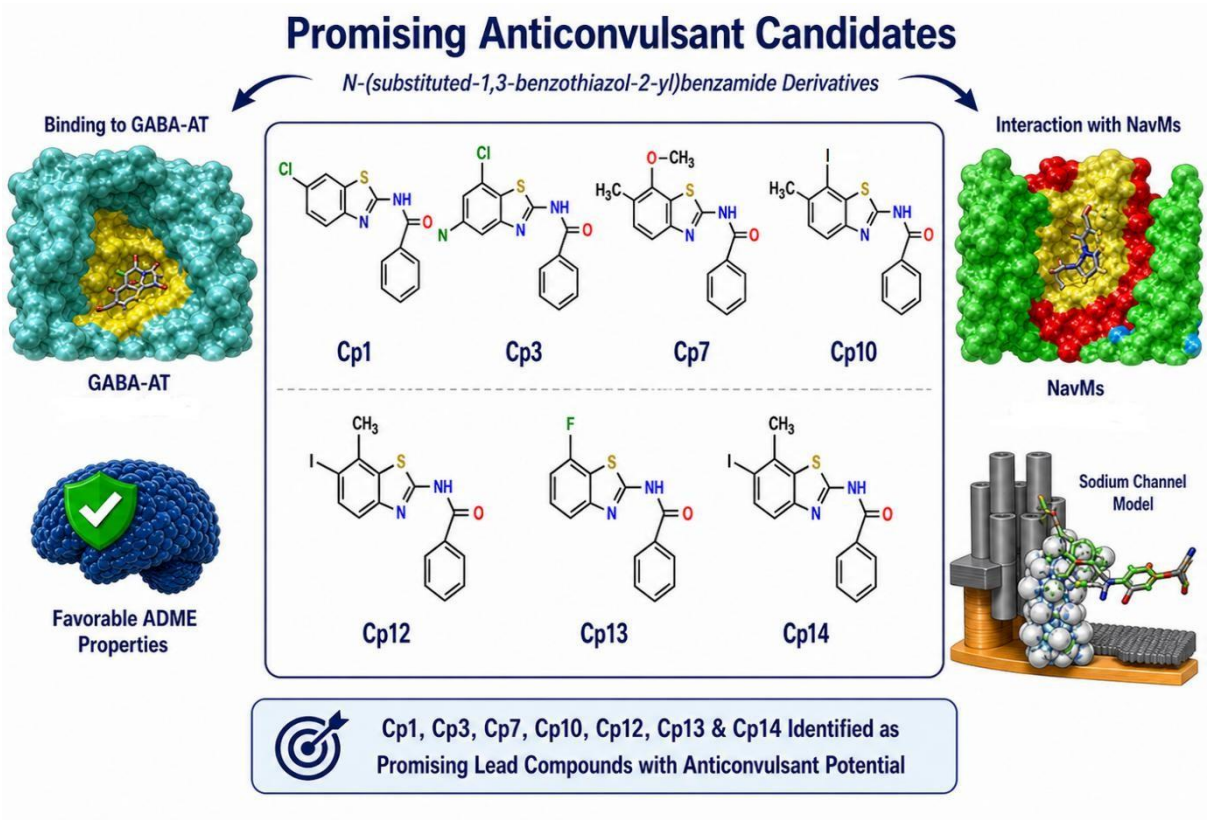

Introduction

Epilepsy is one of the most prevalent chronic neurological disorders, affecting approximately 50 million people worldwide and contributing significantly to premature mortality, particularly in low- and middle-income countries where access to treatment remains limited [1]. Despite advances in antiepileptic drug development, many currently available therapies are associated with significant limitations, including dose-related toxicity, idiosyncratic adverse effects, and poor long-term efficacy. Common side effects such as hepatotoxicity, ataxia, and hematological abnormalities continue to compromise patient compliance and therapeutic outcomes [2, 3]. Despite the development of newer anticonvulsants, first-generation drugs such as phenobarbital, phenytoin, carbamazepine, valproic acid, zonisamide, and clobazam remain widely used despite significant limitations.

Newer agents, such as lamotrigine, topiramate, tiagabine, pregabalin, and stiripentol, are linked to toxicity and limited long-term efficacy [4, 5]. Furthermore, a significant percentage of patients have drug-resistant epilepsy, underscoring the urgent need for safer and more effective therapeutic agents. Despite the rapid development of antiepileptic drugs, rational optimization of anticonvulsant design is still crucial [6, 7]. Finding new scaffolds with better pharmacological properties has been the focus of recent medicinal chemistry efforts. Amides are a class of chemical compounds that have shown significant anticonvulsant potential [8-10]. Their structural characteristics, such as hydrogen bonding capacity and hydrophobic interactions, make them attractive candidates for drug design reports. Benzothiazole derivatives are known to be adaptive pharmacophores with a variety of biological activities, such as antitubercular, antibacterial, anticonvulsant, antidiabetic, anticancer, anthelmintic, analgesic, anti-inflammatory, and antitumor characteristics [11, 12].

γ-aminobutyric acid (GABA) and voltage-gated sodium channels (Navs) are essential for controlling neuronal excitability in the central nervous system. While elevated GABA levels aid in the suppression of seizures, decreased GABA levels can cause convulsions [13]. The first inward current during action potential depolarization is caused by voltage-gated sodium channels, which are linked to increased excitatory (glutamatergic) activity and decreased inhibitory (GABAergic) transmission, both of which contribute to the development of seizures [14, 15]. Using search algorithms and scoring systems to anticipate the best ligand binding, molecular docking is a dependable computational method for researching drug-target interactions. These *in-silico* techniques enhance drug development by offering insightful information about pharmacokinetic characteristics, binding affinity, and interaction mechanisms [16-18]. A two strategy may offer greater therapeutic benefits because the etiology of epilepsy involves both impaired GABAergic inhibition and abnormal sodium channel activity. In order to find promising candidates with enhanced anticonvulsant potential, this study uses molecular docking and *in-silico* ADME analysis to examine the interaction profiles and pharmacokinetic characteristics of N-(substituted-1,3-benzothiazol-2-yl)benzamide derivatives against GABA-AT and activated open sodium channel proteins. The two well-established therapeutic targets GABA-AT and the voltage-gated sodium channel model Nav*Ms* channel were selected based on their critical roles in enhancing inhibitory neurotransmission and suppressing neuronal hyperexcitability.

Materials and Methods

Computational tools

The study utilized the following computational tools: MarvinSketch (v20.20), Spartan ’14 (v1.1.4), AutoDockTools (v1.5.6), UCSF Chimera (v1.11.2), Discovery Studio Visualizer (v20.1.0.19295), and the SwissADME online platform.

Docking analysis

A molecular docking approach was employed as a robust computational method to elucidate the intermolecular interactions between the newly designed compounds and their target receptors, as well as to provide preliminary estimates of their binding affinities.

Ligands Preparation

The MarvinSketch (v20.20) program was used to generate all chemical structures and then saved as an MDL SDfile. These structures were then incorporated into SPARTAN software (Spartan 14). The next stage was to optimize all structures using the molecular mechanics force fields (MMFF) and save them in Sybyl Mol2 format. Ligands were prepared using standard protocols, including structural energy minimization, hydrogen addition, and gasteiger charge computation as discussed previously [19].

Proteins preparation

The protein targets, GABA aminotransferase (GABA-AT; PDB ID: 1OHW) and Nav*Ms* (PDB ID: 5HVX), obtained from the RCSB Protein Data Bank, were prepared using UCSF Chimera (v1.11.2) and AutoDockTools (v1.5.6). Proteins were prepared following the standard protein preparation protocol, which included removal of all water molecules from the complex structures. During a brief relaxation step, hydrogen atoms and charges were added, and the crystal structures were minimized with optimization of the hydrogen-bonding network. Ligands were prepared using a ligand preparation procedure involving energy minimization, hydrogen addition, and charge assignment via the Gasteiger. Docking utilized the cavity detection algorithm, with 10 runs, a population size of 150, a crossover rate of 0.8, and 27,000 maximum generations [19].

Molecular docking evaluation

Process of molecular docking was conducted with the receptor maintained in a rigid conformation, whereas the ligand was permitted to adopt flexible conformation. The virtual

screening software Auto Dock Vina, developed by [20], was utilized for docking. Table 1 presents the grid box parameters for each enzyme.

Table 1: Grid-box dimensions for each enzyme

Enzyme	**PDB**	**Grid box Size**			**Center**		
		X	**Y**	**Z**	**X**	**Y**	**Z**
GABA-AT	1OHW	20	28	18	11.228	-0.47	18.337
NavMs	5HVX	42	46	38	65.379	62.014	17.982

*X, Y, Z represent 3D geometric axes

Docking validation

The docking process was validated prior to screening the test compounds by first removing the co-crystallized ligand from the enzyme structure obtained from the Protein Data Bank and then re-docking it using the same docking parameters with root-mean-square deviation (RMSD) values of 0.9632 Å and 1.02 Å for GABA-AT and Na*Ms* respectively. Successful validation was confirmed when the re-docked pose closely superimposed on the original geometric conformation of the co-crystallized ligand within the active site, as assessed using the virtual screening software (Auto Dock Vina) and the resulting poses were visualized in Discovery Studio 2020 Client [21].

Post docking analysis

Grid box dimensions were established based on the native ligand. Post-docking analyses were carried out using Chimera and Discovery Studio Visualizer to evaluate ligand-enzyme interactions. The leading docking poses were identified, and the conformation exhibiting the essential binding interactions was selected.

Evaluation of pharmacokinetic and ADME properties

Before moving further with cell line and animal experiments, SwissADME, a complete predictive ADME software system (PharmacoPredicta), was built and validated to anticipate pertinent pharmacokinetic and ADME features of chosen hits/lead compounds. Inappropriate pharmacokinetic (PK) characteristics have historically been a primary cause of compound

failure in the latter phases of pharmacological development [22]. This fact was mostly caused by the incapacity to recognize and address subpar pharmacokinetic features found in numerous lead series that were approved for lead optimization. Early knowledge of a compound's absorption, metabolism, distribution, and elimination (ADME) has become crucial in the lead selection and optimization process as high throughput screening, combinatorial chemistry, and parallel synthesis have been used in drug discovery [23, 24]. Notably, [25] groundbreaking study looked at orally active compounds to identify physicochemical ranges that have a high likelihood of being an oral drug (i.e., drug-likeness) [26-28].

Results

Table 2: Molecular structure representation accompanied by compounds bioaffinity scores

S/N	Molecular Structure	Bioaffinity (kcal/mol) for 1OHW	Bioaffinity (kcal/mol) for 5HVX
Compound 1	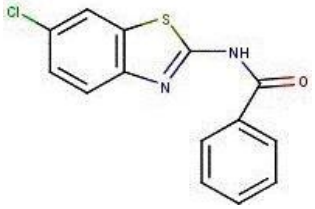 N-(6-chloro-1,3-benzothiazol-2-yl)benzamide (Cp1)	**-6.5**	**-5.6**
Compound 2	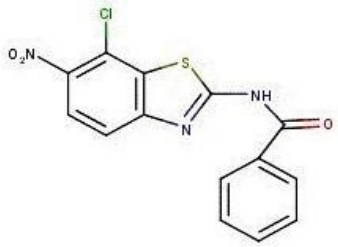 N-(7-chloro-6-nitro-1,3-benzothiazol-2-yl)benzamide (Cp2)	**-6.7**	**-5.2**
Compound 3	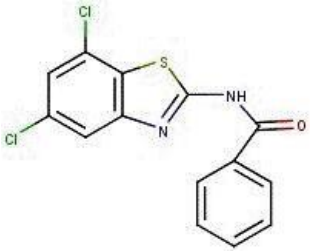 N-(5,7-dichloro-1,3-benzothiazol-2-yl)benzamide (Cp3)	**-7.3**	**-5.5**
Compound 4	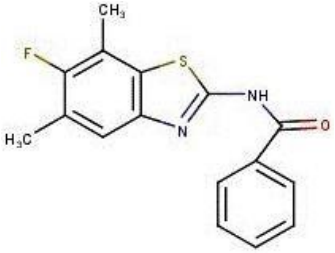 N-(6-fluoro-5,7-dimethyl-1,3-benzothiazol-2-yl)benzamide (Cp4)	**-7.4**	**-6.4**
Compound 5	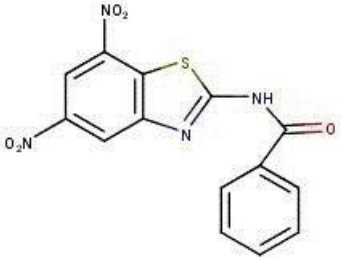	**-7.3**	**-5.6**

Table 2 (*continued*)

	N-(5,7-dinitro-1,3-benzothiazol-2-yl)benzamide (Cp5)		
Compound 6	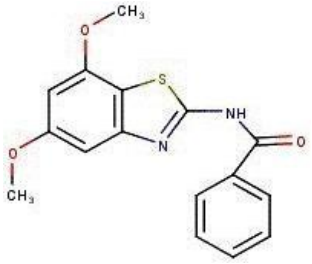	**-7.0**	**-4.6**
	N-(5,7-dimethoxy-1,3-benzothiazol-2-yl)benzamide (Cp6)		
Compound 7	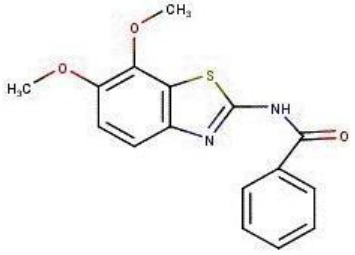	**-7.6**	**-4.9**
	N-(6,7-dimethoxy-1,3-benzothiazol-2-yl)benzamide (Cp7)		
Compound 8	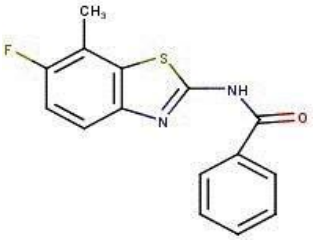	**-7.1**	**-6.2**
	N-(6-fluoro-7-methyl-1,3-benzothiazol-2-yl)benzamide (Cp8)		
Compound 9	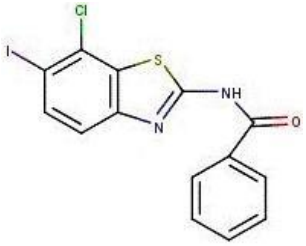	**-6.9**	**-6.2**
	N-(6-fluoro-7-methyl-1,3-benzothiazol-2-yl)benzamide (Cp9)		
Compound 10	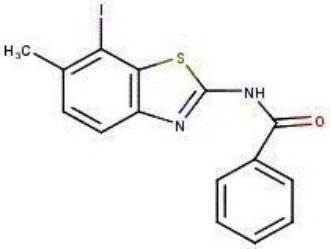	**-7.7**	**-6.3**
	N-(6-fluoro-7-methyl-1,3-benzothiazol-2-yl)benzamide (Cp10)		
Compound 11	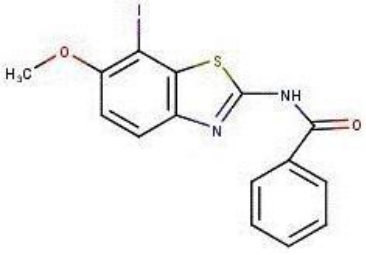	**-7.5**	**-4.8**

	N-(6-fluoro-7-methyl-1,3-benzothiazol-2-yl)benzamide (Cp11)		
Compound 12	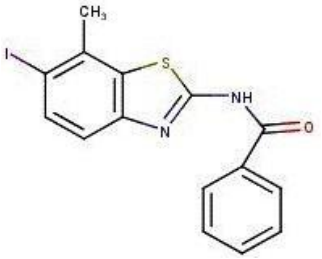	**-6.4**	**-5.5**
	N-(6-fluoro-7-methyl-1,3-benzothiazol-2-yl)benzamide (Cp12)		
Compound 13	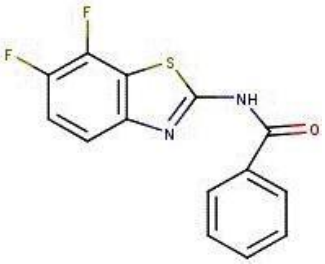	**-6.6**	**-5.4**
	N-(6-fluoro-7-methyl-1,3-benzothiazol-2-yl)benzamide (Cp13)	**-7.4**	**-5.4**
Compound 14	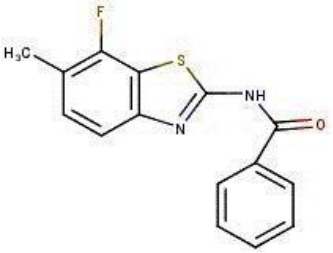		
	N-(6,7-difluoro-1,3-benzothiazol-2-yl)benzamide (Cp14)		
Compound 15	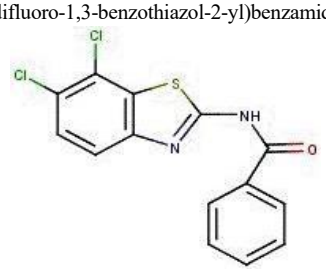	**-7.0**	**-6.6**
	N-(6,7-dichloro-1,3-benzothiazol-2-yl)benzamide (Cp15)		
Reference (Vigabatrin)	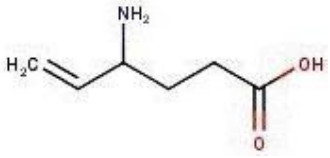	**5.2**	**-**
Reference (Lamotrigine)	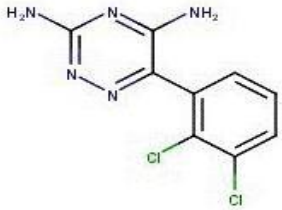	**-**	**5.0**

Note: 1OHW corresponds to γ-aminobutyric acid aminotransferase (GABA-AT), and 5HVX represents the activated sodium channel

Table 3: Docking-based comparison of the binding interactions of Vigabatrin (reference drug) and fifteen N-(substituted-1,3-benzothiazol-2-yl)benzamide derivatives with GABA-AT.

Ligand/ Compound	Amino acid residues forming hydrogen bonds with the ligand	Active-site residues involved in ligand interactions
1	SER137	ILE72, GLY136, ASN140, HIS190, GLY191, ARG192, SER269, GLU270, ASP298, GLN301, LYS329, PHE189, VAL300
2	SER74, SER137, GLY191	GLN71, GLY136, GLU270, GLN301, SER328, PHE189, CYS135, VAL300, LYS329
3	CYS135, SER137, GLY191	CYS135, GLY136, PHE189, HIS190, ARG192, GLU265, GLU270, ASP298, VAL300, GLN301, LYS329
4	HIS190	ILE72, GLY136, ASN140, PHE189, GLY191, ARG192, GLU265, SER269, GLU270, VAL300, GLN301, LYS329
5	SER137, ASN140, GLN301, GLY191, SER269	ILE72, CYS135, GLY136, PHE189, HIS190, ARG192, GLU265, GLU270, ASP298, VAL300, LYS329
6	CYS135, SER137, GLN301, GLU270	GLY136, ASN140, PHE189, HIS190, GLY191, ARG192, GLU265, ASP298, VAL300, SER328
7	CYS135, SER137, GLN301, GLU265, GLU270, ASP298	CYS135, GLY136, ASN140, PHE189, HIS190, GLY191, ARG192, SER269, VAL300, SER328, LYS329
8	ASN140, GLU270, GLN301,	ILE72, GLY136, SER137, PHE189, HIS190, GLY191, ARG192, ASP298, VAL300, LYS329, ARG445,
9	SER137, GLY191	GLN71, ILE72, SER74, CYS135, GLY136, ASN140, PHE189, HIS190, ASP298, VAL300, GLN301, SER328, LYS329
10	GLY136, SER137, GLY191	ILE72, SER74, CYS135, SER137, PHE189, HIS190, ASP298, VAL300, GLN301, SER328, LYS329
11	SER137, GLN301, ASP298	CYS135, GLY136, ASN140, PHE189, HIS190, GLY191, GLU265, GLU270, VAL300, SER328, LYS329
12	CYS135, SER137	CYS135, GLY136, ASN140, PHE189, HIS190, GLY191, ARG192, GLU265, SER269, GLU270, ASP298, VAL300, GLN301, SER328, LYS329
13	SER74, GLY191, LYS329	CYS135GLY136, SER137, ASN140, PHE189, HIS190, ARG192, VAL300, SER328, LYS329
14	SER137, LYS329	CYS135, GLY136, ASN140, PHE189, HIS190, GLY191, GLU270, ASP298, VAL300, GLN301, SER328, LYS329
15	GLY136, SER137, GLY191	GLN71, ILE72, SER74, CYS135, SER137, ASN140, PHE189, HIS190, ASP298, VAL300, GLN301, SER328, LYS329
Reference (Vigabatrin)	SER137, PHE189, GLY191	GLY37, ASN40, HIS190, ARG192, SER269, GLN301, LYS329, VAL300, ASP298

Table 4: Docking-based comparison of the binding interactions of Lamotrigine (reference drug) and fifteen N-(substituted-1,3-benzothiazol-2-yl)benzamide derivatives with activated open sodium ion channel.

Ligand/ Compound	Amino acid residues forming hydrogen bonds with the ligand	Active-site residues involved in ligand interactions
1	GLY76	TRP77, PHE80,LEU125, LEU126, LEU128
2	LEU177, SER179, TRP180	SER181, TRP180, ILE200, ILE203, LEU125
3	TYR153, ALA195	MET148, HIS192, ASN194, PHE198, LEU152, VAL197, TYR153
4	THR139	LEU138, PHE142, LEU168, PHE172, TYR169
5	TRP77	LYS63, PHE80, VAL121, GLN122, LEU125, LEU126, THR139
6	-	GLY76, VAL121, GLN122, TRP77, PHE80, MET108, LEU125, LEU126
7	TYR153, TRP180,PHE198	MET148, LEU152, PRO193, ASN194, HIS192, ALA195, VAL197
8	GLY76	TRP77, LEU79, VAL83, PHE80, VAL121, LEU125, ALA195, VAL197
9	THR139	LEU138, PHE142, TYR143, LEU168, PHE172, TYR169
10	-	ILE144, LEU152, VAL197, PRO201, PHE202, LEU205, PHE80, VAL141, ALA145, THR139
11	-	PHE157, PRO158, GLU159, PRO187, ASN190, TRP160
12	MET175	LEU177, THR207, PHE214, PHE172, VAL210, LEU211
13	MET175	LEU177, THR207, PHE172, PHE214, VAL210, LEU211, THR176
14	TYR153, PHE189	MET148, LEU152, HIS192, PRO193, ASN194, ALA195, VAL197
15	TRP77	GLU10, GLN15, LYS63, SER75, ASN78, SER112, VAL113, ARG119, GLN122, ARG118
Reference (Lamotrigine)	VAL141, PHE198	ALA145, MET148, ILE174, VAL197, PHE198, PRO201, PHE202, LEU205

Table 5: Lipinski's rule-based prediction of oral bioavailability for CNS drugs

Compounds No	Log P	Molecular weight	H-bond donors	H-bond acceptors
Compound 1	3.05	288.75	1	2
Compound 2	2.85	333.75	1	4
Compound 3	3.16	323.20	1	2
Compound 4	3.28	300.35	1	3
Compound 5	1.03	344.30	1	6
Compound 6	1.46	314.36	1	4
Compound 7	1.89	314.36	1	7
Compound 8	2.77	286.32	1	3
Compound 9	3.40	414.65	1	2
Compound 10	3.54	394.23	1	2
Compound 11	2.96	410.23	1	3
Compound 12	3.13	394.23	1	2
Compound 13	3.32	290.29	1	4
Compound 14	3.17	286.32	1	3
Compound 15	3.57	323.20	1	2
Reference (Vigabatrin)	0.28	129.16	2	3
Reference (Lamotrigine)	1.75	256.09	2	3

Note: Note: In accordance with Lipinski's Rule of Five, compounds should possess a molecular weight ≤ 500 Da, logP ≤ 5, no more than 5 hydrogen bond donors, and no more than 10 hydrogen bond acceptors.**Table 6:** Predicted SwissADME parameters of the fifteen compounds were evaluated in comparison to the reference drug.

Compounds No.	GIA	BBB permeant	P-gp
Cp1	High	1	None
Cp2	High	0	None
Cp3	High	1	None
Cp4	High	1	None
Cp5	Low	0	None
Cp6	High	0	None
Cp7	High	0	None
Cp8	High	1	None
Cp9	High	1	None
Cp10	High	1	None
Cp11	High	0	None
Cp12	High	1	None
Cp13	High	1	None
Cp14	High	1	None
Cp15	High	1	None
Reference (Vigabatrin)	High	0	None
Reference (Lamotrigine)	High	0	Enzyme inhibitor

GIA corresponds to gastrointestinal absorption, BBB describes in vivo blood-brain barrier penetration (0 = absent, 1 = present), and P-gp denotes inhibition of P-glycoprotein

Discussion

Molecular docking

GABA-AT represents a promising target for antiepileptic therapy, as selective inhibition of this enzyme increases GABA concentrations in the brain. Vigabatrin (γ-vinyl-GABA), an established antiepileptic drug, has been widely studied using various biochemical techniques, resulting in multiple hypotheses regarding its enzyme-inactivating mechanisms and subsequent elevation of γ-aminobutyric acid levels in central neurons. Based on the best interaction energy with GABA-AT, the docking pose with the highest score for each compounds was chosen [29]. Compounds Cp1, Cp3, Cp7, Cp10, Cp12, Cp13, and Cp14, have substantial binding affinities toward GABA-AT, similar to the reference inhibitor Vigabatrin, according to the docking scores listed in Table 2. Based on a thorough review of the literature, important amino acid residues in the GABA-AT active site were found [10, 30, 31].

The bioaffinity values of the top-ranked compounds docked against γ-aminobutyric acid aminotransferase (GABA-AT) and Nav*Ms* and are shown in Figure 1, emphasizing their respective binding interaction potentials toward both molecular targets. Stronger ligand-

receptor interactions and higher anticipated binding stability are typically indicated by larger negative bioaffinity (binding energy) values in molecular docking studies.

By re-docking vigabatrin into the active site and properly reproducing its binding orientation and interaction profile, as shown in Figures 2and,3 the docking protocol validity was verified. The vigabatrin carbonyl group interacts with Ser137 and Gly191 through conventional hydrogen bonding and carbon hydrogen while the NH group creates salt bridges with Asp298 and convetional hydrogen bonds with Phe189. Alkyl interactions with Val300 and van der Waals contacts with Gly136, Asp140, His190, Arg192, Ser269, Gln301, and Lys329 provide further stability (Figure 2).

A comparison of these findings with the re-docked vigabatrin and its location in the GABA-AT PDB structure is shown in Table 3. Significantly, the best-performing compounds Cp1, Cp3, Cp7, Cp10, Cp12, and Cp14 showed conservation of these important contacts, especially van der Waals interactions with residues like Gly136, His190, Arg192, Gln301, and Lys329 and traditional hydrogen bonding with Ser137. This implies that within the catalytic pocket, the proposed compounds take on binding conformations similar to vigabatrin. Notably, several stabilizing contacts were found, including conventional hydrogen bonding with Gln301 and Gly136 and π-cation interactions for Cp7 and Cp10 with Lys329. According to recent studies highlighting the significance of multi-point interactions in enhancing ligand-enzyme stability and inhibitory activity, these additional interactions may improve binding affinity and specificity. These compounds successfully occupy the GABA-AT active site, confirming their potential as competitive or mechanism-based inhibitors, as further demonstrated by the visual overlap of ligand poses in the docking pictures.

As shown in Table 4, docking studies focusing on the Nav*Ms* channel shed light on the compounds capacity to alter sodium channel function, a crucial mechanism promoting seizure regulation. Despite its utility as a structurally resolved surrogate model, Nav*Ms* remains limited by its prokaryotic homotetrameric architecture, absence of auxiliary β-subunits, and differences

in pore-lining residues relative to mammalian voltage-gated sodium channels. By contrast, the Nav*Ms* structure presented here is the only sodium channel crystal structure to date in which all domains are fully resolved. Notably, it features an activated voltage sensor and a pore gate wide enough to permit sodium ion permeation, aligned with an open-channel conformation, making it suitable for molecular dynamics simulations of ion translocation.

Moreover, the structure reveals previously uncharacterized interdomain interactions, providing a structural framework for understanding the coupling between voltage-sensor activation and pore-gate opening. The Nav*Ms* structure thus delivers key mechanistic insights into sodium channel function, including: (i) the physical linkage between voltage-sensor activation and pore-gate opening; (ii) the C-terminal domain plays an important role in stabilizing the open-channel conformation and regulating gating dynamics; (iii) the identification of a conserved interaction motif shared by prokaryotic and eukaryotic sodium channels; and (iv) defining structural features that distinguish sodium channels from other ion channel families. These findings suggest that the Nav*Ms* channel may serve as a suitable model for characterizing and identifying blockers of eukaryotic sodium channels [32].

Electrophysiological studies of Nav*Ms* channels containing mutations in surrounding residues have validated the proposed binding site. In addition, literature reports have identified key amino acid residues involved in the Nav*Ms* binding site [33-35].

Re-docking of the reference drug Lamotrigine (Figures 4 and 5) reproduced characteristic interactions, including conventional hydrogen bonding with Val141 and Phe198, π–π stacking with Phe198, and hydrophobic interactions involving residues such as Ile144, Met148, and Phe202. These results are consistent with electrophysiological and crystallographic investigations that identify the conventional sodium channel binding pocket. Among the produced derivatives, Cp10, Cp13, and Cp14 showed binding modes that were similar to lamotrigine, occupying the same binding site and displaying similar interaction profiles. With residues like Ala145, Ile144, and Phe202, these compounds generated important

hydrophobic and π-alkyl interactions that are known to aid in ligand stability within the channel pore. The general interaction pattern indicates that these compounds may be useful sodium channel blockers, even if slight variations were noted, such as carbon hydrogen bonding with Phe198 rather than typical hydrogen bonding. Recent research demonstrating the significance of hydrophobic and aromatic interactions in securing ligands within sodium channel binding sites supports this observation.

Pharmacokinetic and ADME Studies

Tables 5 and 6 summarize the compounds pharmacokinetic properties, which show that the majority of derivatives have desirable drug-like features. Most of the compounds have good oral bioavailability potential, according to Lipinski's criteria for CNS drugs (Table 5). Significantly, ten compounds Cp1, Cp3, Cp4, Cp5, Cp9, Cp10, Cp12, Cp13, Cp14, and Cp15 were predicted to penetrate the blood-brain barrier (BBB), an essential requirement for the activity of central nervous system. These compounds fits into a suitable physicochemical region for CNS-active drugs, as further shown by the graphical representation of ADME features in Figure 6. These results align with known factors that influence BBB permeability, such as molecule size, polarity, and lipophilicity [36-41].

Furthermore, unlike lamotrigine, which is known to be influenced by P-gp-mediated transport, none of the compounds were anticipated to interact significantly with P-glycoprotein (P-gp). P-glycoprotein is necessary for lamotrigine to cross the blood-brain barrier, underscoring the involvement of this transporter in the inadequate CNS absorption of numerous antiepileptic drugs [42-44].

Additionally, the majority of compounds met Lipinski's rule for CNS drugs, indicating favorable drug-likeness and oral bioavailability [36-38]. The ADME profiles, supported by graphical analyses, place the lead compounds within the optimal physicochemical space for CNS-active drugs, balancing lipophilicity, polarity, and molecular weight [36-41].

Conclusion

Based on the molecular docking results, several N-(substituted-1,3-benzothiazol-2-yl)benzamide derivatives demonstrated favorable interactions within the active sites of the two target proteins. Seven compounds (Cp1, Cp3, Cp7, Cp10, Cp12, Cp13, and Cp14) exhibited promising binding affinity toward GABA-AT, while three compounds (Cp10, Cp13, and Cp14) also showed effective interactions with Nav*Ms*. In addition, these derivatives displayed favorable ADME characteristics necessary for efficient central nervous system delivery. Among these compounds, Cp1, Cp3, Cp7, Cp10, Cp12, Cp13, and Cp14 were identified as the most promising lead candidates, exhibiting notable potential as anticonvulsant agents.

List of Abbreviations

GABA-AT: Gamma-aminobutyric acid-aminotransferase

Nav*Ms*: Voltage-gated Sodium Channels Protein from *Magnetococcus marinus*

PDB: Protein Data Bank

RCSB: Research Collaboratory for Structural Bioinformatics

Cp: Compound

Navs: Voltage-gated Sodium Channels

CNS: Central Nervous System

MMFF: Molecular Mechanics Force Fields

BBB: Blood Brain Barrier

ADME: Absorption Distribution Metabolism and Elimination

PK: Pharmacokinetic

2D: Two-Dimensional

3D: Three-Dimensional

GIA: Gastrointestinal Absorption.

Authors' Contribution

Conceptualization: A.R.; **Methodology:** A.R.; **Investigation:** A.R.; **Data curation:** A.R., A.Y.I., A.M.M., H.S.H., A.H.N., M.G.M., R.B., M.S., I.J.M.; **Formal analysis:** A.R., A.Y.I., A.M.M., H.S.H., A.H.N., M.G.M., R.B., M.S., I.J.M.; **Visualization:** A.Y.I.; **Supervision:** A.Y.I., A.M.M., H.S.H., A.H.N., M.G.M.; **Writing—original draft:** A.R.; **Writing—review and editing:** A.Y.I., A.M.M., H.S.H., A.H.N., M.G.M., R.B., M.S., I.J.M. All authors have read and approved the published version of the manuscript.

ORCID's

Ahmed Rufa'i[1*]:0000-0002-1882-3916

Abdullahi Y. Idris[2]: 0000-0003-4313-1572

Aliyu M. Musa[2]: 0000-0001-7985-9157

Halimatu S. Hassan[2]: 0000-0001-6333-0910

Asma'u H. Nasiru[2]: 0000-0002-8172-8284

Mohammed G. Magaji[3]: 0000-0001-7107-4267

Rabiu Bako[4]: 0000-0003-1515-5171

Muhammad Sa'idu[5]: 0009-0003-2252-2176

Isah J. Muhammad[6]: 0009-0005-1723-932X

Availability of Data and Materials

All data utilized in the current research were developed through experiments using computation and are included in this manuscript, and further can be obtained from the corresponding authors.

Conflicts of Interests

The authors report no conflicts of interest in relation to this study.

Funding

No external funding was received for this research.

Ethics Approval and Consent to Participate

Ethics approval is not applicable.

Acknowledgment

The authors sincerely acknowledge the Department of Pharmaceutical and Medicinal

Chemistry, Faculty of Pharmaceutical Sciences, Ahmadu Bello University, Zaria, Nigeria, for providing essential research facilities and support for this study. The authors also appreciate the Department of Pharmaceutical and Medicinal Chemistry, Gombe State University, Gombe, Nigeria and the Department of Pharmaceutical and Medicinal Chemistry, Kaduna State University, Kaduna, Nigeria for providing additional research facilities that contributed to the successful completion of this work.

AI-Declaration

The authors acknowledged the use of Quilbot AI tools during the preparation of this manuscript solely for language enhancement, grammar correction, and manuscript readability improvement. This tool was not used in the study concept or design, data collection, experimental computation, results interpretation or formulation of scientific conclusion. All intellectual content, scientific interpretations, and conclusions presented in this manuscript is the sole responsibility of the authors. The authors have critically reviewed, checked, and approved the final version of the manuscript and accept full responsibility for its accuracy, integrity, and originality.

References

1. WHO. Intersectoral global action plan on epilepsy and other neurological disorders 2022–2031. *Geneva*, **2023**. https://www.who.int/news/item/12-01-2022-draft-intersectoral-global-action-plan-on-epilepsy-and-other-neurological-disorders-2022-2031 (accessed 6 April, 2022).
2. Fonseca-Barriendos, D.; Frías-Soria, C.L.; Pérez-Pérez, D.; Gómez-López, R.; Borroto-Escuela, D.O.; Rocha, L. Drug-resistant epilepsy: Drug target hypothesis and beyond the receptors. *Epilepsia*, **2022**, 1, S23-S33. doi: 10.1002/epi4.12539.
3. Benny, F.; Oh, J.M.; Kumar, S.; Abdelgawad, M.A.; Ghoneim, M.M.; Abdel-Bakky, M.S.; Kukerti, N.; Jose, J.; Kim, H.; Mathew, B. Isatin-based benzyloxybenzene derivatives as monoamine oxidase inhibitors with neuroprotective effect targeting neurogenerative disease treatment. *Royal Society of Chemistry Advances*, **2023**, 13(50), 35240-35250. doi: 10.1039/d3ra07035b.

4. Giulia, S.; Arianna, G.; Luca, B. The Development of Epilepsy Following CNS Viral Infections: Mechanisms. *Current Neurology and Neuroscience Report*, **2024**, 25(1), 2. Doi: 10.1007/s11910-024-01393-4.
5. Taiki, M.; Toru, H.; Yuichi, N.; Shuhei, I.; Naoki, H.; Ichiro, K. Tolerability of perampanel: A retrospective study at the department of psychiatry. *Epilepsy and Behavior*, **2024**, 156, 109797. Doi: 10.1016/j.yebeh.2024.109797.
6. Tafere, M.B. Recent Progress in the Development of New Antiepileptic Drugs with Novel Targets. *Annals of Neurosciences*, **2023**, 30, 15. Doi: 10.1177/09727531231185991.
7. Mehdi, V.; Majid, G.; Saeed, K.; Zahra, Z.K.; Helia, A; Fatemeh, S; Sholeh, A.; Fereshteh, T.A.; Asieh, H.; Majid, J.; Hamid, I.; Saeed, E. Design, synthesis, and structure-activity relationships of five-membered heterocyclic incorporated aryl(alkyl)azoles: From antiproliferative thiazoles to safer anticonvulsant oxadiazoles. *Bioorganic Chemistry*, **2024**, 108-117. Doi: 10.1016/j.bioorg.2024.108117.
8. Grover, G.; Pal, R.; Bhatia, R.; Yar, M.S.; Nath, R.; Singh, S. Design, synthesis and pharmacological evaluation of aryl oxadiazole linked 1,2,4-triazine derivatives as anticonvulsant agents. *Medicinal Chemistry Reserve*, **2022**, 31: 781-93. Doi: 10.21203/rs.3.rs-1301847/v1.
9. Alhamzani, A.G.; Yousef, T.A.; Abou-Krisha, M.M.; Raghu, M.S.; Yogesh, K.K.; Prashanth, M.K. Design, synthesis, molecular docking and pharmacological evaluation of novel triazine-based triazole derivatives as potential anticonvulsant agents. *Bioorganic & Medicinal Chemistry Letters*, **2022**, 77, 129042.
10. Walaa, H.A.; Mohamed, S.A.M.; Marawan, A.E.; Alyaa, F.H.; Rasha, M.H. Design and synthesis of novel cycloalkanecarboxamide parabanic acid hybrids as anticonvulsants. *Medicinal Chemistry Research*, **2023**, 1-18. https://doi.org/10.1007/s00044-023-03166-z.
11. Gaurav, K.; Sanjay, S.; Manisha, N.; Abhishek, S. An In-Depth Analysis of Benzothiazole Derivatives: Structure, Properties, and Applications. *International Journal of Scientific*

Research in Science and Technology, **2024**, 11(5), 17-42. Doi: https://doi.org/10.32628/IJSRST24114141.

12. Qiang, W.; Tomas, N.; Lars, E; Kálmán, J.S. Sulfenofunctionalization of Chiral α-Trifluoromethyl Allylboronic Acids: Asymmetric Synthesis of SCF3, SCF2 R, SCN and SAr Compounds. *Angewandte Chemie International and Discovery*, **2024**, 61(46), e202210509. doi: 10.1002/anie.202210509.
13. Punam, S.; Parameswari, A.; Ravikumar, K.; Amarendarm, R.M. Identification of novel C-15 fluoro isosteviol derivatives for GABA-AT inhibition by in silico investigations. *Journal of Molecular Modeling*, **2023**, 29(3), 76. doi: 10.1007/s00894-023-05479-7.
14. Bai, F.; Song, Y.; Cao, Y.; Ban, M.; Zhang, Z.; Sun, Y.; Feng, Y.; Li, C. Scorpion Neurotoxin Syb-prII-1 Exerts Analgesic Effect through Nav1.8 Channel and MAPKs Pathway. *International Journal of Molecular Science*, **2022**, 23(13), 7065. doi: 10.3390/ijms23137065.
15. Kanemura, H. Therapeutic Strategies in Children with Epilepsy: A Quality-of-Life-Related Perspective. *Journal of Clinical Medicine*, **2024**, 13(2), 405. doi: 10.3390/jcm13020405.
16. Hasan, M.R.; Alsaiari, A.A.; Fakhurji, B.Z.; Molla, M.H.R.; Asseri, A.H.; Sumon, M.A.A.; Park, M.N; Ahammad, F.; Kim, B. Application of mathematical modeling and computational tools in the modern drug design and development process. *Molecules*, **2022**, 27(13): 41-69.
17. Garg, A; Dewangan, H.K. Recent advances in drug design and delivery across biological barriers using computational models. *Letters in Drug Design and Discovery*, **2022**, 19(10), 865-876. Doi: 10.2174/1570180819999220204110306.
18. Niu, Y.; Lin, P. Advances of computer-aided drug design (CADD) in the development of anti-Azheimer's-disease drugs. *Drug Discovery Today*, **2023**, 28, 103665.
19. Rufa'i, A.; Idris, A. Y.; Musa, A. M.; Hassan, H. S.; Nasiru, A. H.; Magaji, M. G. Molecular docking and *In-Silico* pharmacokinetic analysis of 1,3-benzothiazole-2-amine derivatives

as anticonvulsants. *Journal of Taibah University Medical Sciences*, **2025**, 20(5), 629-642. https://doi.org/10.1016/j.jtumed.2025.08.002.

20. Trott, O.; Olson, A. J. AutoDock Vina: improving the speed and accuracy of docking with a new function, efficient optimization, and multithreading. *Journal of Computational Chemistry*, **2010,** 31(12), 455-61. http://vina.scripps.edu.
21. Eldeeb, M.; Sanad, E. F.; Ragab, A.; Ammar, Y. A.; Mahmoud, K.; Ali, M. M.; Hamdy, N. M. Anticancer effects with molecular docking confirmation of newly synthesized isatin sulfonamide molecular hybrid derivatives against hepatic cancer cell lines. *Biomedicines*, **2022**, 10(3), 722. doi: 10.3390/biomedicines10030722.
22. Girija, B.; Ajay, V.S.; Preeti, B.; Tulika, R.; Sweta, V.N.; Amruta, S.; Rajendra, P.; Peter, L.; Andreas, L.; Christopher, J. O.; Michael, W. S. Decoding Tattoo and Permanent Makeup Pigments: Linking Physicochemical Properties to Absorption, Distribution, Metabolism, and Elimination Profiles Using Quantitative Structure–Activity Relationship (QSAR)-Based New Approach Methodologies (NAMs). *Advanced Intelligent Discovery*, **2025**. https://doi.org/10.1002/aidi.202500027.
23. Marzouk, A.A.; Bass, A.K.; Ahmed, M.S.; Abdelhamid, A.A.; Elshaier, Y.A.; Salman, A.M. Design, synthesis and anticonvulsant activity of new imidazolidindione and imidazole derivatives. *Bioorganic chemistry*, **2020**, 101, 104020.
24. Siomone, Q.P.; Philipe, O.F.; Jose, E.G.; Vinicius, G.M.; Kathia, M.H. Recent Advances in the Prediction of Pharmacokinetics Properties in Drug Designed Studies: A Review. *ChemMedChem*, **2022**, 17, 1-13. Doi.org/10.1002/cmds.202100542.
25. Lipinski, C.A.; Lombardo, F.; Dominy, B.W.; Feeney, P.J. Experimental and computational approaches to estimate solubility and permeability in drug discovery and development settings. *Advanced Drug Delivery Reviews*, **2012**, 64, 4-17. https://doi.org/10.1016/j.addr.2012.09.019.
26. Swagat, K.D.; Archana, M.; Swaroop, S. Phytochemical characterization and bioactivity

assessment of Avicennia officinalis L. bark extracts. *Analytical Chemistry Letters*, **2024**, 14 (3), 369-381, Doi: 10.1080/22297928.2024.2361772.

27. Pooja, R.H.; Rupali, A.M.; Ravindrakumar, L.B.; Kanchan, A.H.; Supriya, S.B. Advance and opportunities in nanoparticle drug delivery for central nervous system disorders: A review of current advances. *GSC Biological and Pharmaceutical Sciences*, **2024**, 27(03), 044-058.
28. Matoševi´c, A.; Opsenica, D.M.; Bartoli´c, M.; Marakovi´c, N.; Stoilkovi´c, A.; Komatovi´c, K.; Zandona, A.; Žunec, S.; Bosak, A. Derivatives of Amodiaquine as Potent Human Cholinesterases Inhibitors: Implication for Treatment of Alzheimer's Disease. *Molecules*, **2024**, 29, 53-57. https://doi.org/10.3390/ molecules29225357.
29. Nikhil, C.; Shreyes, R.M.; Shambanagouda, R.M.; Krishna, V.S.; Vimal, K.; Ajay, V. S.; Areejit, S. TICToK: A comprehensive knowledgebase of tattoo ink chemicals and investigation of their associated toxicities and regulations. *BioRsiv*, **2025**. https://doi.org/10.1101/2025.08.02.668261.
30. Aboutabi, M.E.; Hassan, R.M.; El-Azzouny, A.A.; Aboul-Enein, M.N.; Abd-Allah, W.H. Design and synthesis of novel parabanic acid derivatives as anticonvulsants. *Bioorganic Chemistry*, **2020**, 94, 103473.
31. Abd-Allah, W.H.; Osman, E.E.A.; Anwar, M.A.; Attia, H.N.E; Moghazy, S.M. Design, synthesis and docking studies of novel benzopyrone derivatives as anticonvulsants. *Bioorganic Chemistry*, **2020**, 98, 103738.
32. Choudhary, S.; Dubey, A.; Singh, A.; Zamboni, P.; Gupta, N.; Singh, R. Engineering the microenvironment: advanced biomaterials for humanized in vitro immunotoxicology and carcinogenicity assessment. *Exploration of BioMat-X*, **2025**, 2, 101351. https://doi.org/10.37349/ebmx.2025.101351.
33. Bagneris, C.; Decaen, G.P.; Naylor, E.C; Pyride, C.D.; Nobeli, I.; Clapham, E.D.; Wallace, B.A. Prokaryotic NavMs channel as a structural and functional model for eukaryotic

sodium channel antagonism. *Bentham Science Publishers*, **2014**, 23 (111), 8428-8433. Doi: 10.1073/pnas.1406855111.

34. Sait, L.G.; Sula, A.; Ghovanloo, M.R.; Hollingworth, D.; Ruben, P.C.; Wallace, B.A. Cannabidiol interactions with voltage-gated sodium channels. *Elife*, **2020**, 9, e58593.
35. McCollum, MM.; Megan, L; Shingo, I.; Leo, C.T.N.; Louise, F.K.; Eduardo, G; My, C.T,; Thuy, N.V.; Grant, B.F.; Karl, A.S; Rachel, E.M.; Paul, G.D. Targeting the tamoxifen receptor within sodium channels to block osteoarthritic pain. *Cell Reports*, **2022**, 40, 111248. https://doi.org/10.1016/j.celrep.2022.111248.
36. Hassan, P.; George, R.L. Medicinal chemical properties of successful central nervous system drugs. *NeuroRx*, **2005**, 2(4), 541-53. DOI: 10.1602/neurorx.2.4.541.
37. Bisht, N.; Singh, B.K. Structure based virtual screening, molecular docking studies and modification of hydantoin nucleus analogues as anticonvulsant. *Indian Journal of Chemistry*, **2018**, 57, 1514-1525.
38. Verma, S.D.; Passerat, C.E.; Malkani, S.; Juran, C.M.; Boyko, V.; Costes, S.V.; Cekanaviciute, E. Astrocytes regulate vascular endothelial responses to simulated deep space radiation in a human organ-on-a-chip model. *Frontiers in Immunology*, **2022**, 13, 864923. Doi: 10.3389/fimmu.2022.864923.
39. Fru, C. G.; Serab, K.; Yunus, B.; Jenifer, R. N. K.; Valaire, Y. M.; Jason, B. T. K.; Junior, F. M.; Melvis, A. C.; Semiha, Y. G.; Aponglen, A.; Armelle, T. M.; Victor, K.; Farzana, S. Antibacterial flavonoids from *Tetrapleura tetraptera* (Fabaceae) fruit pulp, *in silico* studies. *South African Journal of Botany*, **2025**, 180, 96-106. https://doi.org/10.1016/j.sajb.2025.02.026.
40. Yunus, B.; Semiha, Y.; Aslı, Y. K.; Fru C.G.; Erhan, O.; Ibrahim, D.; Ahmet, Z. T. Cytotoxicity of *Dysphania botrys* L. Extracts Against HEPG2 and SAOS-2, In Vitro and In Silico. *Chemistry and Biodiversity*, **2025**, 22 (12), e01615.

https://doi.org/10.1002/cbdv.202501615.

41. Yunus, B.; Aybek, Y.; Fru C. G.; Busran, S.; İbrahim, D. Green Synthesised Silver Nanoparticle From *Cotoneaster horizontalis*, In Vitro and In Silico Antibacterial Properties. *Chemistry and Biodiversity*, **2026**, 23 (1), e02265. https://doi.org/10.1002/cbdv.202502265.
42. Li, J.; Zhang, Z.; Zhang, B.; Yan, X.; Fan, K. Transferrin receptor 1 targeted nanomedicine for brain tumor therapy. *Biomaterials Science*, **2023**, 11(10), 3394–3413.
43. Ping, H.; Ding, D.; Zhu, G.; Wang, J.; Zhang, J. Advancements in the application of nanotechnology for the management of epileptic seizures. *Acta Epileptologica*, **2024**, 6, 23. https://doi.org/10.1186/s42494-024-00171-6.
44. Villa, M.; Wu, J.; Hansen, S.; Pahnke, J. Emerging Role of ABC Transporters in Glia Cells in Health and Diseases of the Central Nervous System. *Cells*, **2024**, 13, 740. https://doi.org/10.3390/cells13090740.

Figures:

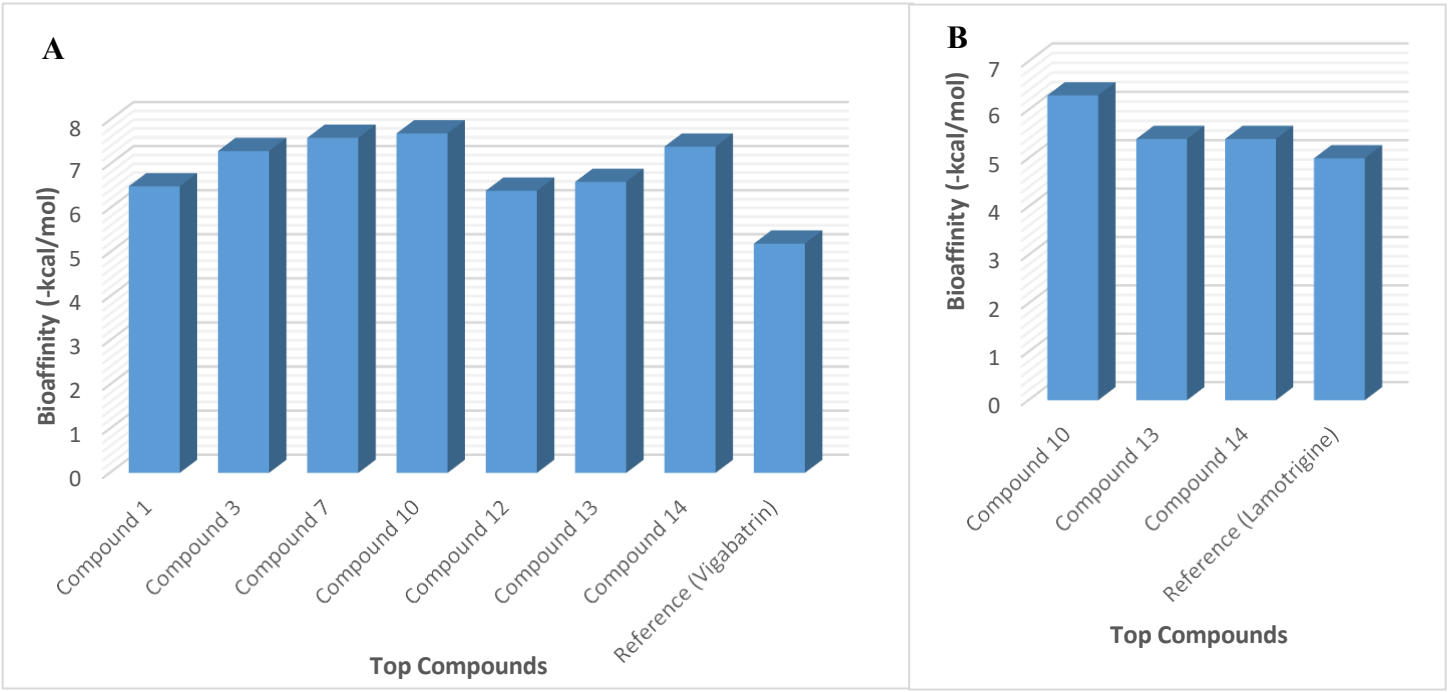

Figure 1: Binding affinity values of the top-ranked compounds toward (**A**) GABA-AT and (**B**) Nav*Ms*.

A

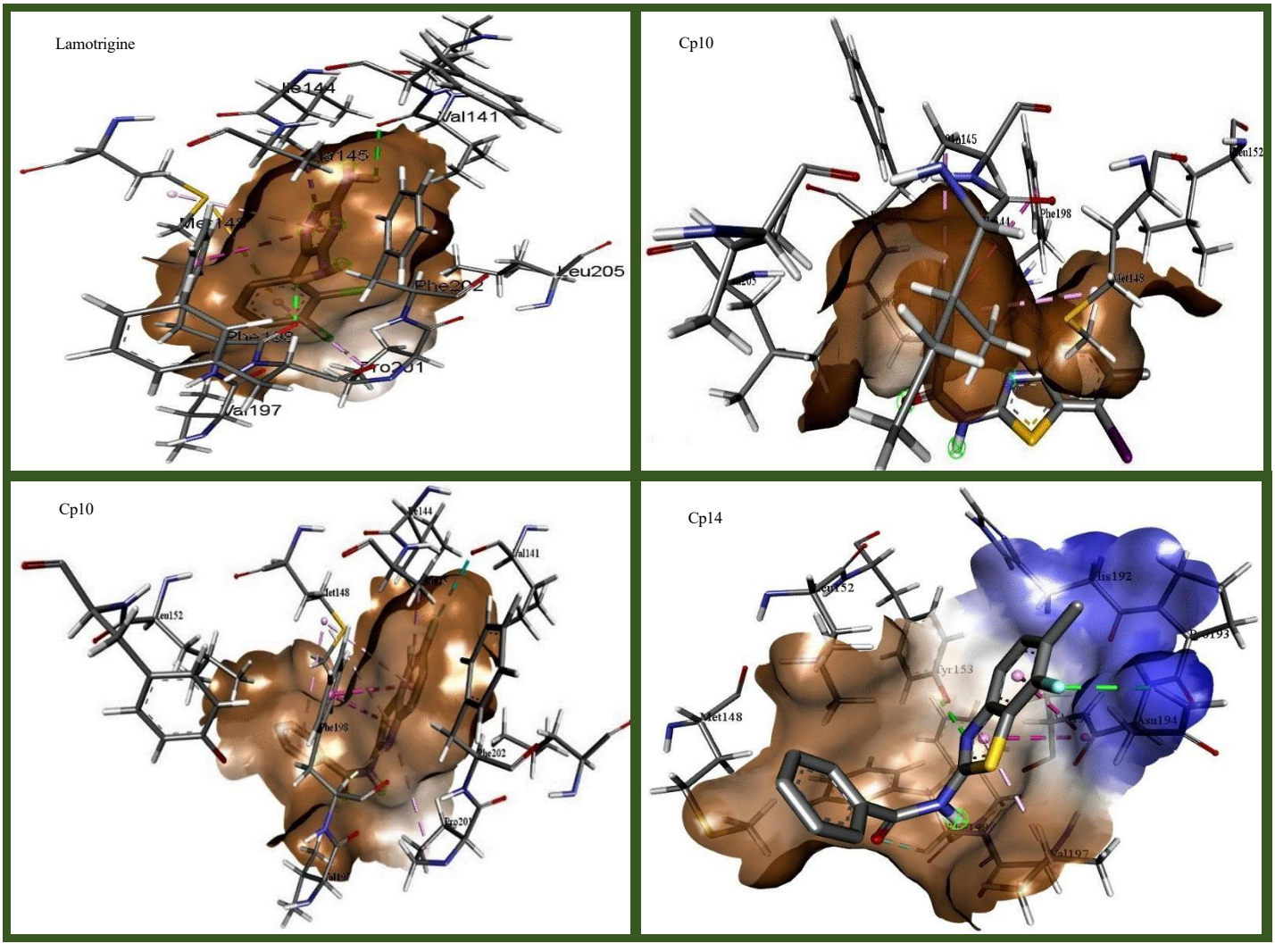

Figure 2: Structural depiction of 3D interactions between Lamotrigine and selected compounds (Cp10, Cp13, and Cp14) at the Nav*Ms* active site.

A

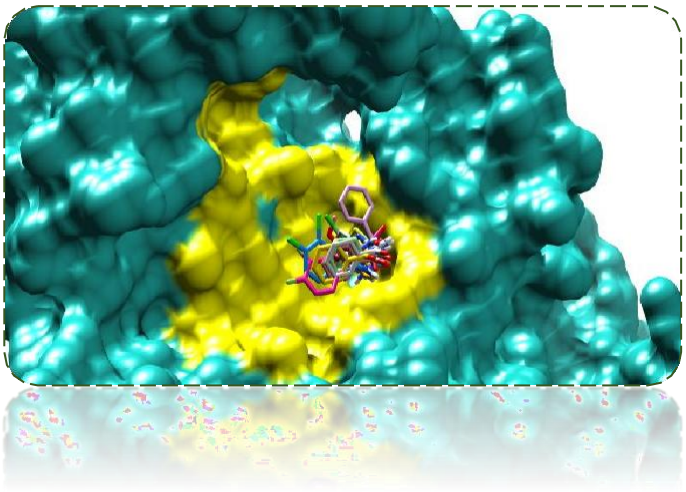

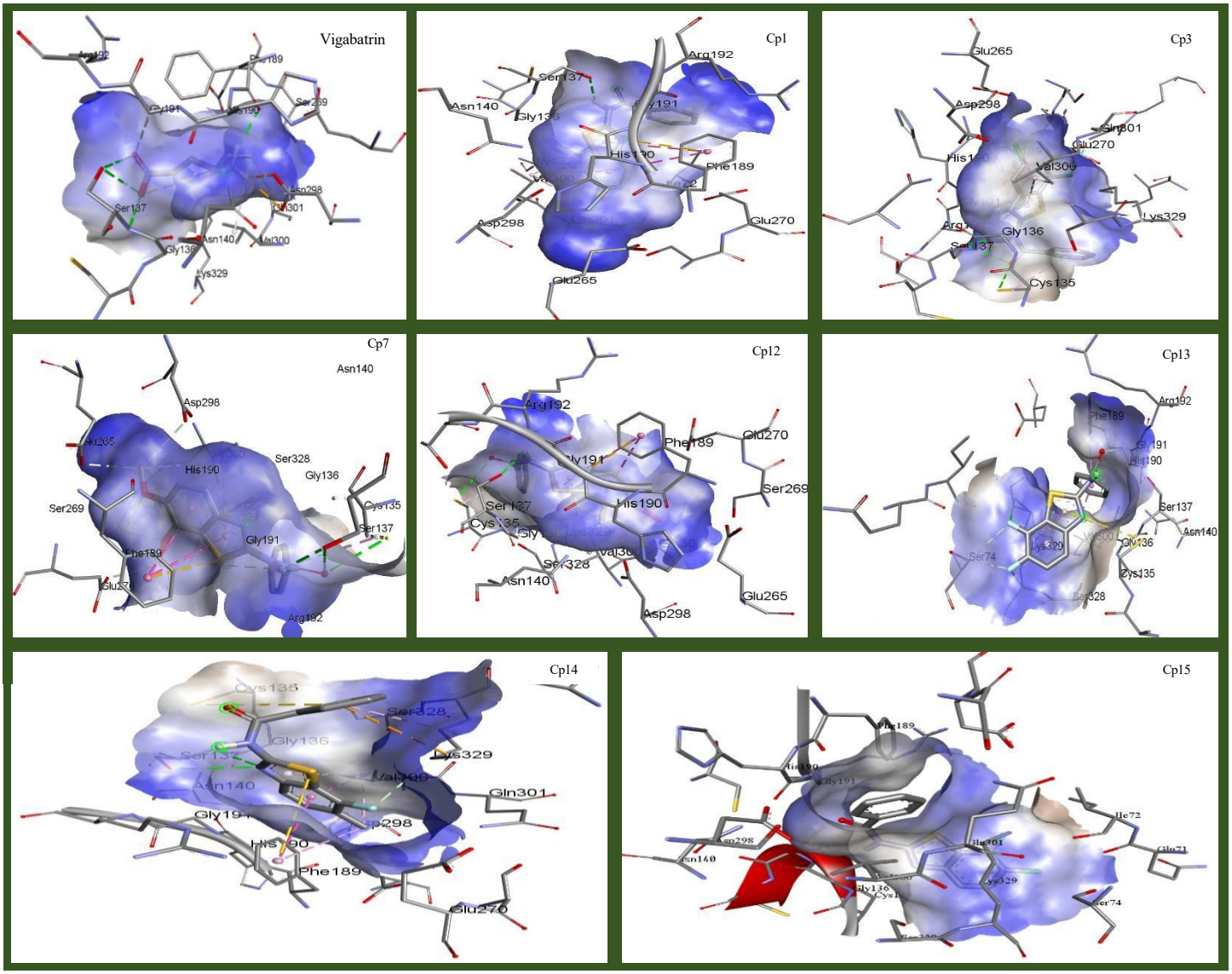

Figure 3: Structural depiction of 3D interactions between Vigabatrin and selected compounds (Cp1, Cp3, Cp7, Cp12, Cp13, Cp14, and Cp15) at the GABA-AT active site.

A

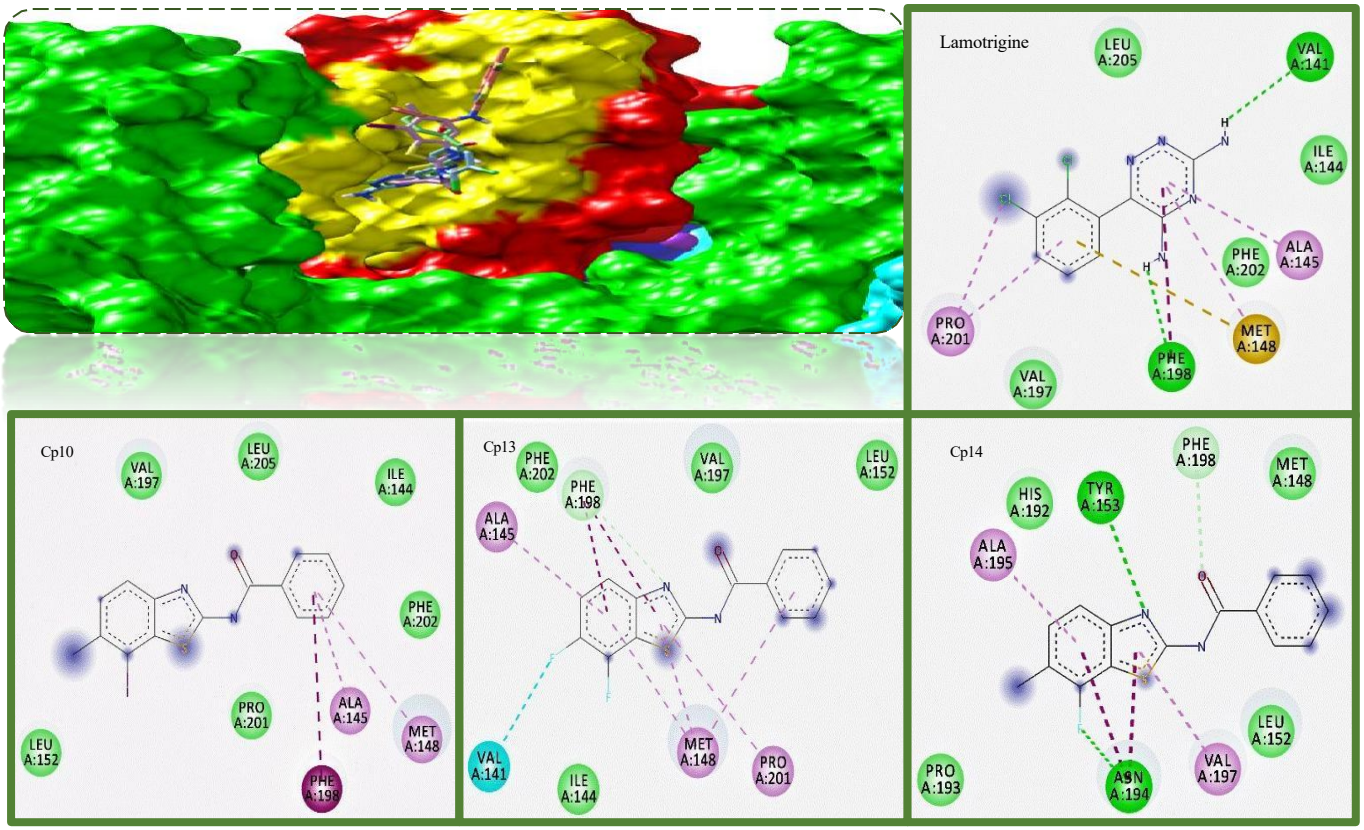

Figure 4: Comparison of molecular surface and 2D interaction patterns of Lamotrigine and selected compounds (Cp10, Cp13, and Cp14) within the Nav*Ms* active site. (**A**) Structural representation of Nav*Ms*.

A

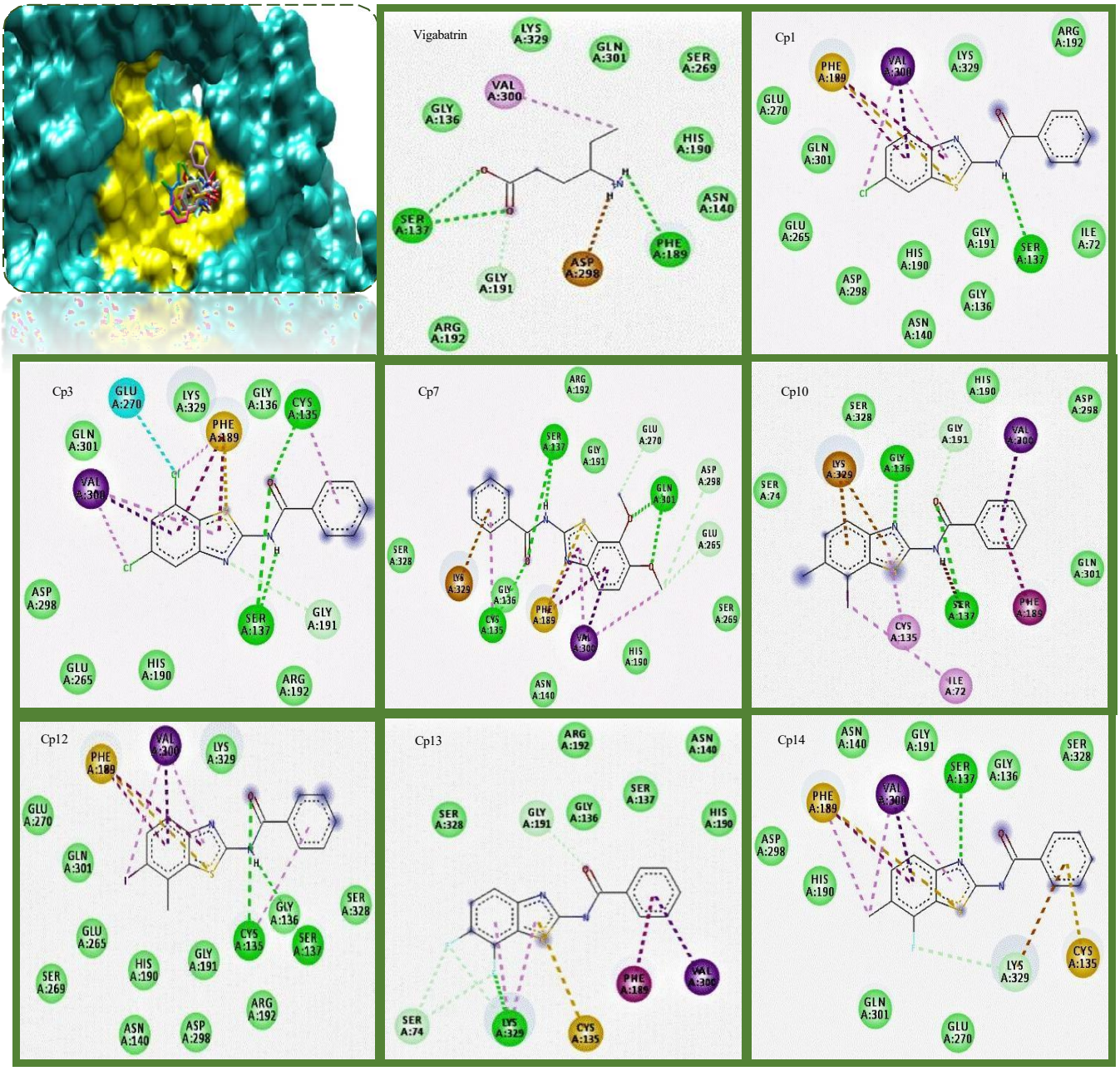

Figure 5: Comparison of molecular surface and 2D interaction patterns of Vigabatrin and selected compounds (Cp1, Cp3, Cp7, Cp10, Cp12, Cp13, and Cp14) within the GABA-AT active site. (**A**) Structural representation of GABA-AT.

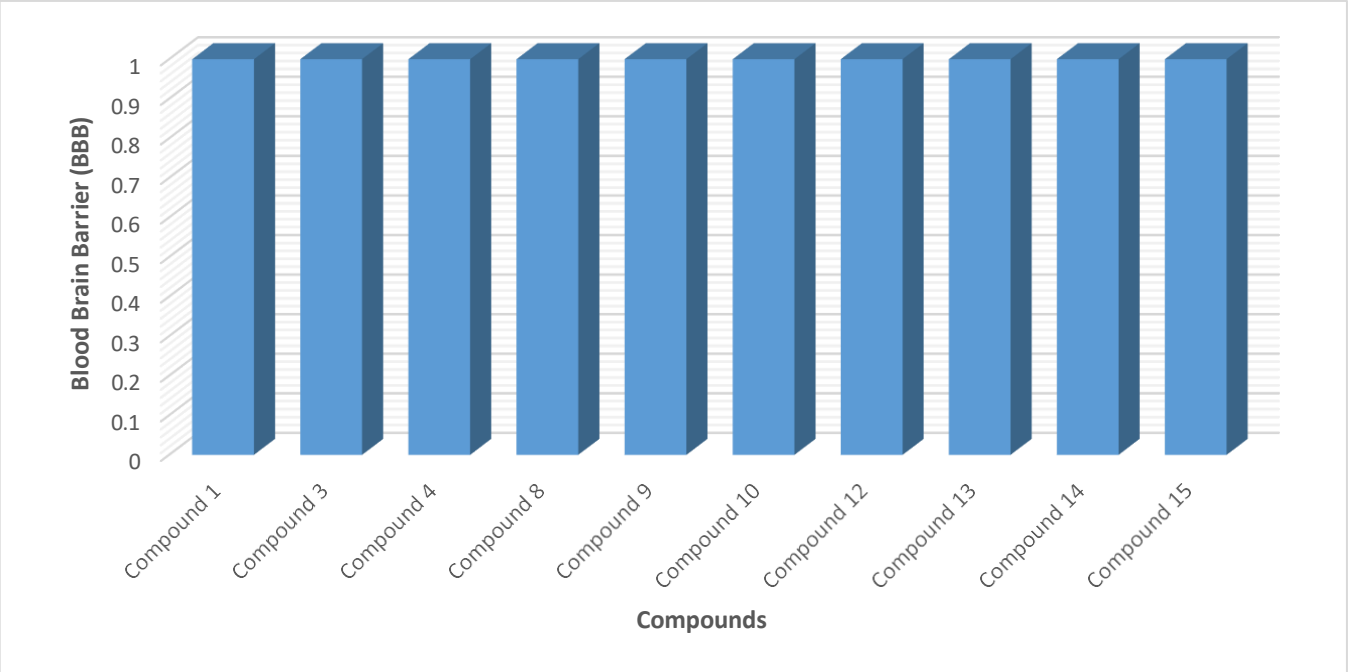

Figure: 6: Graphical representation of compound exhibiting blood-brain barrier permeability